Tuijin Jishu/Journal of Propulsion Technology
ISSN:1001-4055
Vol. 44 No.2 (2023)

Investigative Studies on Thermal performance of Heatpipe with suspended Nanoparticles

Dr. Prasad CSMV[1], Dr. Venkataraja Mohan S D[2], Supritha R. M[3], Dr. Shivaprasad H[4*]

[1]*Professor, Department of Civil Engineering, SJBIT, Kengeri, Bengaluru-560060, Karnataka, India*

[2]*Professor, Department of Civil Engineering, Dr. Ambedkar Institute of Technology, Bengaluru-56, Karnataka, India*

[3] *Assistant Professor, Department of Civil Engineering, Dr. Ambedkar Institute of Technology, Bengaluru-56, Karnataka, India*

[4*]*Assistant Professor, Department of Civil Engineering, University of Visvesvaraya College of Engineering, (First State Autonomous University on IIT Model), Bengaluru-560056, Karnataka, India*

Corresponding Author: Dr. Shivaprasad H[4*]

***Abstract*:**This paper presents an experimental investigation regarding the use of solid nanoparticles added to water as a working fluid. Tests were made on a thermosyphon heat pipe. The experiment was performed in order to measure the temperature distribution and compare the heat transfer rate of the thermosyphon heat pipe with nanofluid and with DI-water. The iron oxide nanoparticles were obtained by the laser pyrolysis technique. The tested concentration level of nanoparticles is 0%, 2%, and 5.3%. Results show that the addition of 5.3% (by volume) of iron oxide nanoparticles in water presented improved thermal per-formance compared with the operation with DI-water.

Keywords: *Nanoparticles Laser pyrolysis, Thermosyphon heat pipe Heat transfer rate.*

1. Introduction

The investigation of thermosyphon heat pipes and their applica- tions into thermal engineering are known for years, being used in various applications, such as heat exchangers, electronics cooling, chemical engineering, waste heat recovery, power generation, air conditioning systems, water heater, and solar collectors.

Thermosyphon heat pipes are passive heat transfer devices with high effective thermal conductivity. The effective coefficient of thermal conductivity of a thermosyphon heat pipe can be orders of magnitude higher than that of highly conductive solid materials, such as copper.

The thermosyphon heat pipe can be divided into three sections:

- The evaporator which is located near the heat source;
- The condenser which is located near the heat sink;
- The adiabatic section in the middle of the thermosyphon heat pipe.

A thermosyphon is similar to a heat pipe. Thermal input at the evaporator region vaporizes the working fluid and this vapor trav- els to the condenser section through the inner core of the heat pipe. At the condenser region, the vapor of the working fluid con- denses, and the latent heat is rejected via condensation. The con- densate returns to the evaporator by means of capillary action in the wick. As previously mentioned there is liquid vapor

equilib- rium inside the heat pipe. When thermal energy is supplied tothe evaporator, this equilibrium breaks down as the working fluid evaporates. The generated vapor is at a higher pressure than that provided through the section for the vapor space. Vapor condenses releasing its latent heat of vaporization to the heat sink (Fig. 1a). Thermosyphons transfer heat in exactly the same way as the heat pipe by evaporation followed by condensation. However wickless is present to aid liquid transport from the condenser back to the evaporator, and thus the evaporator must be located vertically below the condenser, gravity will then ensure that the condensate returns to the evaporator (Fig. 1b).

The idea of dispersing solid particles into liquids initially came from James Clerk Maxwell. The use of particles of nanometer dimension was first continuously studied by a research group at the Argonne National Laboratory around a decade ago. Compared with suspended particles of millimeter-or-micrometer dimensions, nanofluids show better stability, and rheological properties, dra- matically higher thermal conductivities, and no penalty in pressure drop. Several published literature have mainly focused on the pre- diction and measurement techniques in order to evaluate the ther- mal conductivity of nanofluids (see for instance Ref. [1]).

Recent works have shown that the presence of the nanoparti- cles in thermosyphons and heat pipes causes an important enhancement of their thermal characteristics [2–20]. Different nanoparticles such as silver [2,7,10,12,18], oxide copper [4,8,14,15,17,19], alumina [17,19,20], diamond [5,11], titanium [2,6], nick- el oxide [9], gold [13], and iron oxide [16] have been utilized within the thermosyphons and heat pipe working fluid. The improved thermal performance is observed through a reduction in thermal resistance [2,5–8,10,12,13], a drop in the temperature gradient [2,11,12], an increase of efficiency [3,18–20], and an enhancemen

in the overall heat transfer coefficient [9]. Also, in some studies[4,8,18,20],theexistenceofanoptimumamountandafilledratioofnanofluidshasbeenestablished.

Nomenclature

c_p	specific heat (J/Kg K)	DT	the mean temperature difference (K)
M_C	mass flow rate of the cooling water (Kg/m³)	T_{E1}, T_{E2}	inlet and outlet temperatures from evaporator section (K)
R	heat pipe thermal resistance (K/W)		
Q	heat transfer rate (W)	T_{C1}, T_{C2}	inlet and outlet temperatures from condenser section (K)
Q_{max}	maximum heat transfer rate (W)		

Iron oxide nanoparticles are of considerable research interest as effective catalysts, engineering applications, magnetic recording media, and attractive materials for biological and medical applica- tions. Researches concerning the use of the iron oxide nanoparti- cles in thermosyphon heat pipes have not been reported.

According to the Fe-O phase diagram [21], there are three equi- librium iron oxides: FeO, Fe3O4 and a-FeO. In addition, Fe may form metastable oxides, including c-Fe2O3, which exists at high temperatures in a broad composition range and transforms into the equilibrium oxide a-Fe2O3.

In this work, an experimental investigation employing iron oxide nanoparticles is performed in order to study the thermal per- formance of a thermosyphon heat pipe. The iron oxide nanostruc- tures were obtained by the laser pyrolysis technique [22]. Three cases, for iron oxide nanoparticles in water with volume concen- trations 0%, 2%, and 5.3% are considered. The results are finally compared with the thermal performance of the thermosyphon heat pipe filled with DI-water.

2. Experiments

2.1 Synthesisandcharacterizationofironoxidenanofluids

The test nanofluids were obtained by dispersing iron oxide nanoparticles (National Institute for Laser, Plasma and RadiationPhysics – Romania) in pure water. The iron oxide nanoparticles, with mean sizes of about 4–5 nm were prepared by the CO2 laser co- pyrolysis of iron pentacarbonyl Fe(CO)5 (vapors) and air. The method is based on the resonance between the emission of a CW CO2 laser line and the infrared absorption band of a gas

precursor and on subsequent heating of precursors by collisional energy transfer.

The synthesis has been carried out in a flow reactor that has been described in detail earlier. Thefocused continuous-wave CO2 laser radiation (k = 10.6 lm) was orthogonally crossed with thereactant gas stream that was admitted to the center of the reac- tion cell through a nozzle system.Since the Fe(CO)5 molecules do not absorb the CO2 laser radiation, C2H4 (ethylene) was used as sensitizer. The nucleated particles formed during reaction were en- trained by the gas stream to the cell exit where they were collected in a trap. Due to both the milliseconds time scale in which particles are formed and the high heating/cooling rates evolving near the reaction zone (well defined by the focused laser spot), the freshly nucleated particles are rapidly quenched to very low mean diame- ters (typically below 10 nm in case of iron compounds) and narrow size distributions.

The variation of the experimental conditions allow for monitor- ing the dimension and the morphology of the synthesized nano- powders. For the preparation of the iron oxide samples used is this work, the main parameters namely the laser power, the reac- tor pressure, the relative flow of the oxidizing agent (air), and the flow of ethylene (as Fe(CO)5 carrier) were optimized and fixed at the following values: 35 W, 300 mbar, 70 sccm, and 145 sccm, respectively.

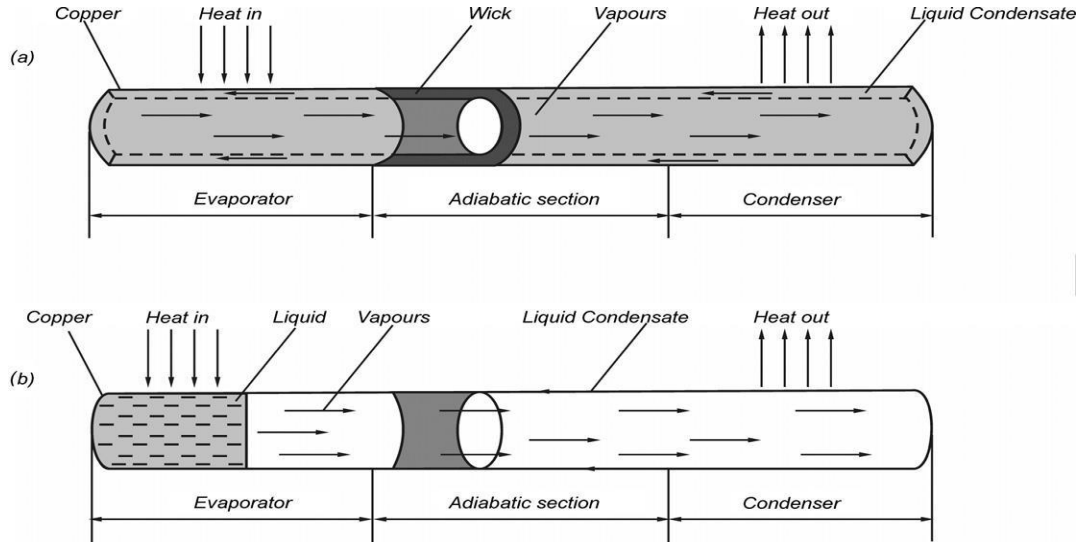

Fig.1.Theconstructionandtheprincipleofoperationfor:(a)heatpipe;(b)thermosyphonheatpipe.

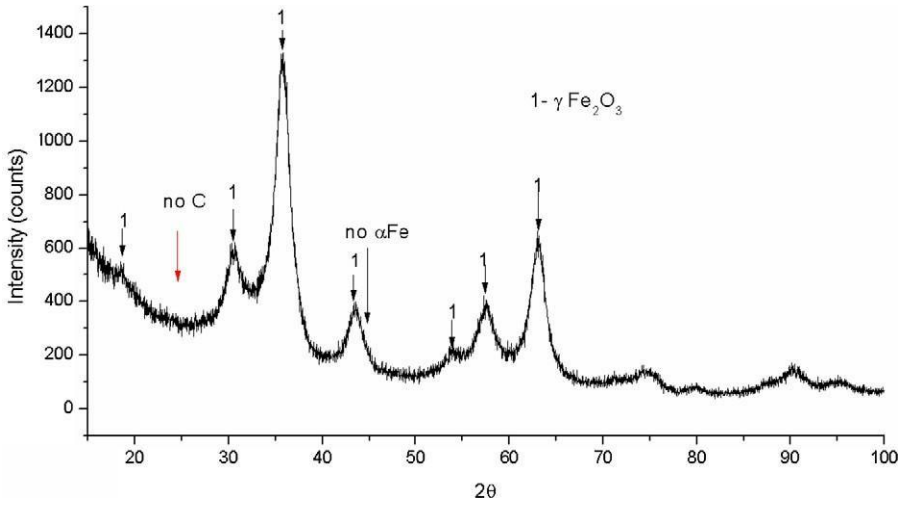

Fig. 2. X-ray diffractogram for the iron oxide nanoparticle

Fig. 2 showed displays the XRD (X-ray diffraction) diagram of the as synthesized iron oxide nanoparticles. In spite of their rela- tive broadness, the diffractions peaks suggest that maghemite/magnetite (c-Fe2O3/Fe3O4) is the major iron oxide phase. The estimated value of the unit cell parameter a approaches the standard value for the maghemite phase (with a = 8.3515 Å, JCPDS 39-1346). The broadness of the diffraction lines is associated with the forma- tion of very small particles as well as with a high degree of struc- tural/crystallographic disorder.

TEM (transmission electron microscopy) analysis of the nano iron oxide sample reveals an almost polycrystalline morphology (Fig. 3). Faceted particles with coalescent features are observed. The histogram of the particle size distribution (lognormal fitted) is presented in the left inset of Fig. 3. The maximum is found at xc = 4.5 nm. The narrow particle distribution points to nearly mon- odispersed in size particles.

HRTEM (high – resolution transmission electron microscopy) analysis was performed on many different domains of the nano- composite and is presented in Fig. 4. The interface between two nanocrystals may be observed. From the indicated square areas, the Fourier transform images are presented as insets. The left-side nanocrystal displays the characteristics of the cubic structure of a maghemite crystal (SG: P4 (3) 32), as demonstrated by the mea- sured interplanar distances d321 = 0.224 nm and d400 = 0.200 nm.The orientation of the right-hand crystal reveals the lattice fringes corresponding to the maghemite planes (113) (d113 = 0.253 nm)and(400) (d400 = 0.204 nm), respectively.

2.2 Experimentalsetup

An experimental system was setup in order to measure the temperature of the thermosyphon heat pipes (Fig. 5). In the exper- iment, the outer diameter and the length of the copper thermosy- phon heat pipe are 15 and 2000 mm, respectively. All the other geometric parameters for the thermosyphon heat pipe are given in Table 1.

The temperatures distribution at the wall of the thermosyphon heat pipe was measured with a P-100-typethermo- resistance of

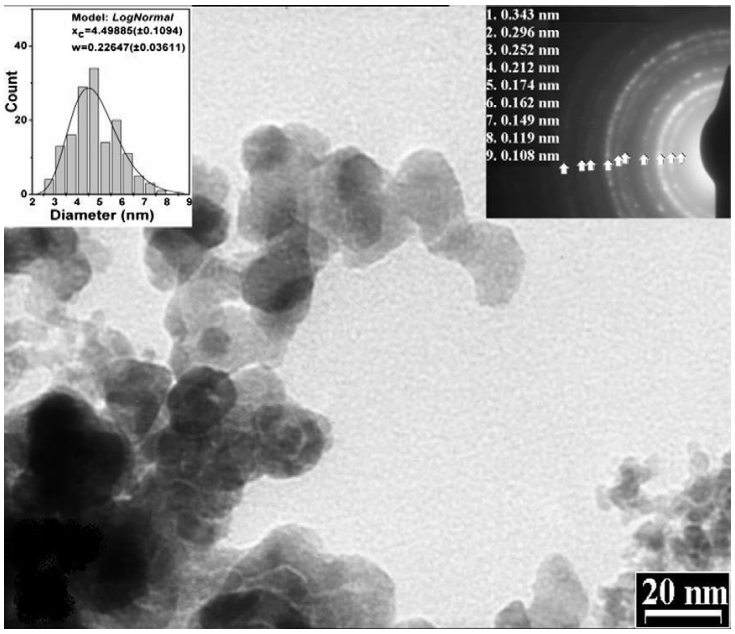

Fig.3.TEManalysis,deducedhistogram(leftinset)andSAEDanalysis(rightinset)forironoxides.

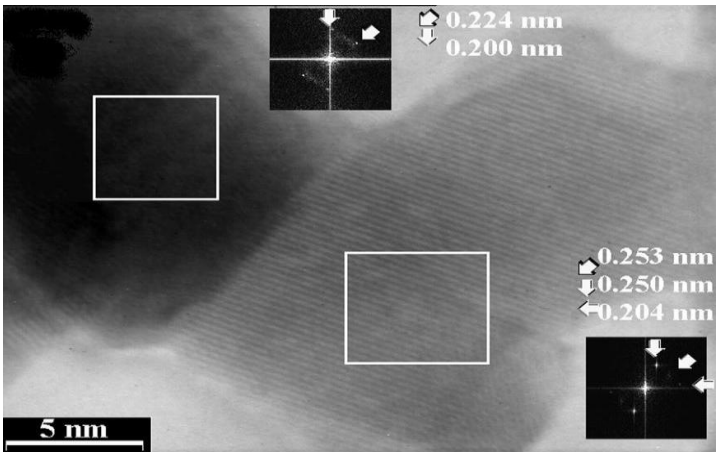

Fig. 4. HRTEM images, for the iron oxide sample:(a) isolated monocrystals, showing the separation interface and (b) agglomerated nanoparticles. In both images, space representations of Fourier transform are displayed.

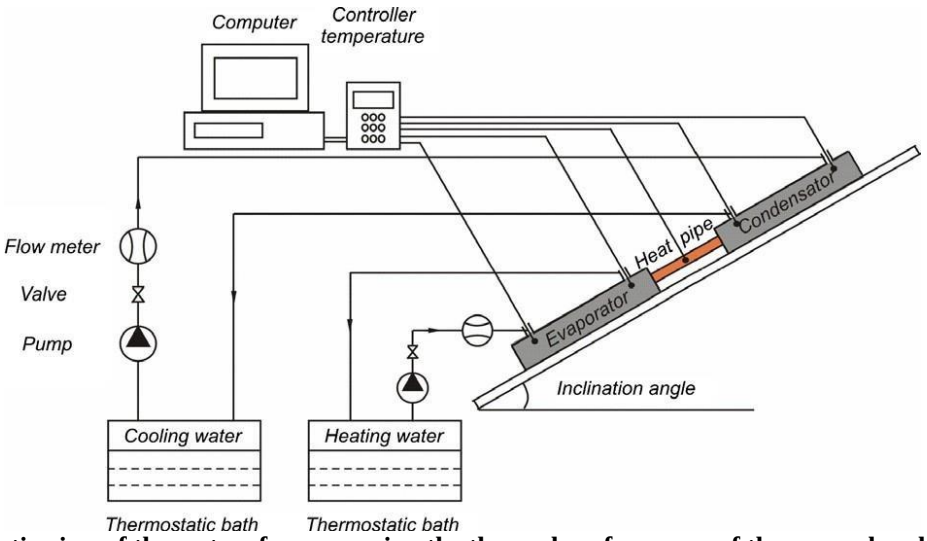

Fig. 5. Schematic view of the system for measuring the thermal performance of thermosyphon heat pipes with nanofluids.

Table 1. Heat pipe experimental configuration.

Heatpipecontainer	Copper
Heatpipelength	2000[mm]
Evaporatorlength	850[mm]
Condenserlength	850[mm]
Adiabaticsection	300[mm]
Outerdiameter	15[mm]
Wallthickness	0.7[mm]
Liquidfilledvolume	12%
Inclinationangle	45°and90°

6 mm in diameter. In total five thermo-resistances were attached on the thermosyphon heat pipe wall, i.e. four at both the evapora- tion section and the condensation section, and one at the adiabatic section. The uncertainty in temperature measurements was±0.1 ℃.The temperature of the heating water from the evaporator sec- tion was kept constant by a thermostatic bath (GD 120-S26) and the operating temperature was varied between 50 and 95 ℃. The temperature of the cooling water from the condenser was kept constant at 20 ℃ through a thermostatic bath (Haake C10 – P5/ U) with an uncertainty of ±0.04 ℃. The adiabatic operating tem- peratures ranged from 34 to 40 ℃, thus: 34–35 ℃ for DI-water, 35– 40 ℃ for iron oxide nanoparticles. Thermosyphon heat pipes were insulated by foamed polystyrene of 10 mm thickness. The inlet and outlet temperatures from evaporator and condensers sections and the mass flow rates of the cooling water were also measured.

All the tests so far conducted have been performed at inclina- tion angles of 45° and 90° (vertical), respectively, and with the mass flow rate of 0.0482509 kg/s (DI-water), 0.0504955 kg/s (2% vol. nanoparticles) and 0.053659 kg/s (5.3% vol. nanoparticles). The inclination angle of the thermosyphon heat pipe was definedas the angle between the horizontal axis and the surface of the thermosyphon heat pipe.

The heat transfer rate can be calculated by Eq. (1) as follows:

$$Q = M_c c_p (T_{C2} - T_{C1}) \quad [W] \qquad (1)$$

The thermal resistance of the thermosyphon heat pipe can be determined by the following equation:

$$R = \frac{DT}{Q_{max}} \quad \frac{K}{W} \qquad (2)$$

Where the temperature difference between the mean temperature of condenser and evaporator is:

$$DT = \frac{T_{E1} + T_{E2}}{2} - \frac{T_{C1} + T_{C2}}{2} \quad [K] \qquad (3)$$

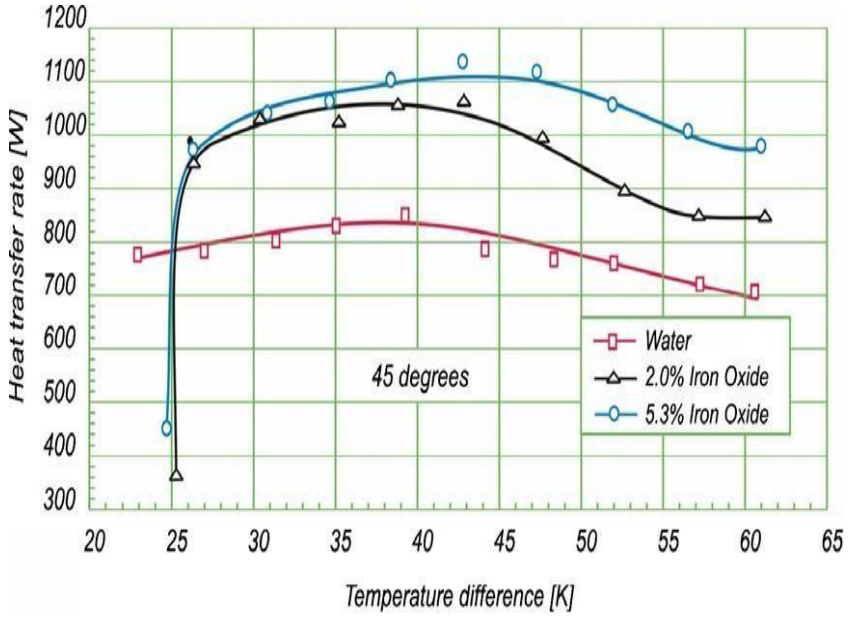

Fig. 6. Heat transfer rate distributions for different concentration levels and an inclination angle 45°.

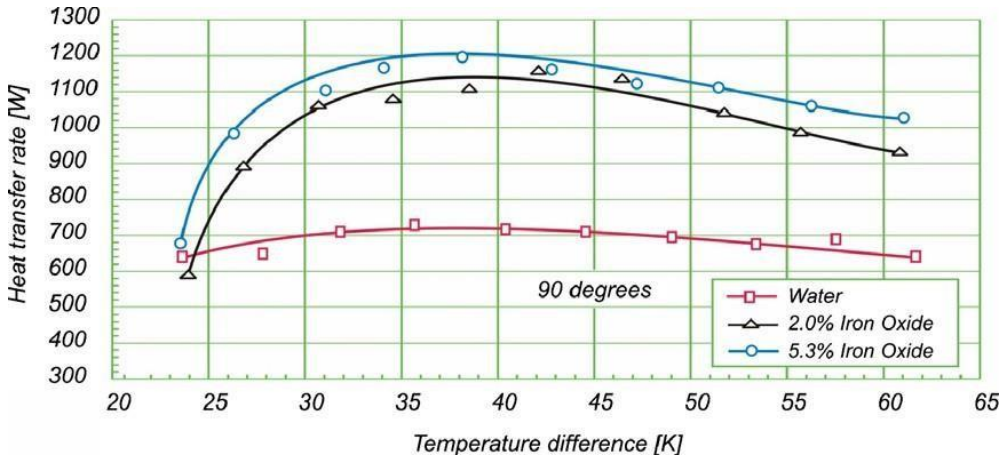

Fig.7.Heattransferratedistributionsfordifferentconcentrationlevelsandaninclinationangleof90°.

3. Results and Discussions

Fig. 6 shows the performance curves of thermosyphons heat pipes with different working fluids and an inclination angle of 45°. Comparing with the water thermosyphon heat pipe, remark- able increases of the heat transfer rate were observed in the case of the thermosyphon heat pipe with different concentration levels of iron oxide nanoparticles. For example, the presence a 2% iron oxide nanoparticles in water results in an increase of the heattransfer rate with 19%, and for 5.3% iron oxide nanoparticles in water the heat transfer rate increase with 22.2%.

Fig. 5 shows the thermal performance of the thermosyphonheat pipe, but for an inclination angle of 90°. In this figure, an increase of heat transfer rate of 39% is obtained for a 2% iron oxideThe reason for reducing the thermal resistance of thermosy- phon heat pipe can be explained as follows. A major thermalresistance of thermosyphon heat pipe is caused by the formation of vapor bubble at the liquid–solid interface. A larger bubble nucle- ation size creates a higher thermal resistance that prevents the transfer of heat from the solid surface to the liquid [23]. The sus- pended nanoparticles tend to bombard the vapor bubble during the bubble formation. Therefore, it is expected that the nucleation size of the vapor bubble is much smaller for the fluid with sus- pended nanoparticles than that without them.

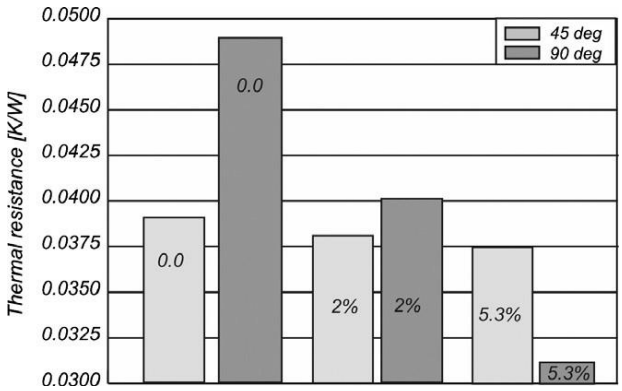

Fig. 8. The effect of different nanoparticle concentration levels on the thermosy- phon heat pipe thermal resistance.

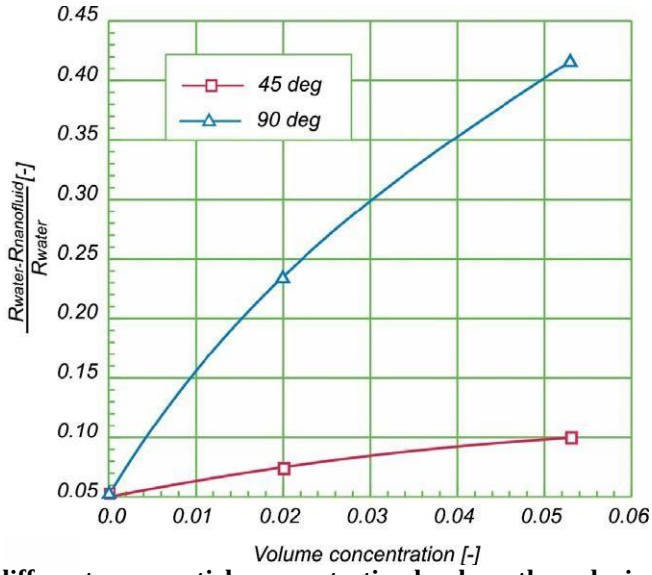

Fig. 9. The effect of different nanoparticle concentration levels on the reducing rate of thermal resistance.

4. Conclusions

This paper deals with the thermal enhancement of the ther- mosyphon heat pipe performance, using iron oxide – nanofluidas the working fluid. In the present case, the DI-water with diluted iron oxide nanoparticles in thermosyphon heat pipes was experi- mentally tested. The two inclination angles of the testing ther- mosyphon heat pipe are 45° and 90° (vertical).

Conclusions may be drawn from the results of the performance tests as follows:

- The more iron oxide nanoparticles were dispersed in the work- ing fluid enhancement of the thermosyphon heat pipe perfor- mance expressed by of the performance curves (heat transferrate as a function of the temperature difference);
- The heat transfer rate increases, in the case of the thermosy- phon heat pipe with iron oxide nanoparticles, as the inclinationangle increases.
- The thermal resistance of the thermosyphon heat pipes with nanoparticle solution is lower than that with DI-water. It is shown that the thermal resistance decreases as the concentration increases;
- Results indicate that the iron oxide nanofluid has remarkable potential as working fluid for thermosyphon heat pipe of higher thermal performances.

5. References

[1] U.S. Choi, Enhancing thermal conductivity of fluids with nanoparticles, ASME FED 231 (1995) 99–103.

[2] S.W. Kang, W.C. Wei, S.H. Tsai, S.Y. Yang, Experimental investigation of silver nanofluid on heat pipe thermal performance, Appl. Therm. Eng. 26 (2006) 2377– 2382.

[3] P. Naphon, D. Thongkum, P. Assadamongkol, Heat pipe efficiency enhancement with refrigerant–nanoparticles mixtures, Energy Convers. Manage. 50 (2009) 772–776.

[4] X.F. Yang, Z.H. Liu, J. Zhao, Heat transfer performance of a horizontal microgrooved heat pipe using CuO nanofluid, J. Micromech. Microeng. 18 (2008) 035038.

[5] H.B. Ma, C. Wilson, Q. Yu, K. Park, U.S. Choi, M. Tirumala, An experimental investigation of heat transport capability in a nanofluid oscillating heat pipe, J. Heat Transfer 128 (2006) 1213–1216.

[6] P. Naphon, P. Assadamongkol, T. Borirak, Experimental investigation of titanium nanofluids on the heat pipe thermal efficiency, Int. Commun. Heat Mass Transfer 35 (2008) 1316–1319.

[7] S.W. Kang, W.C. Wei, S.H. Tsai, C.C. Huang, Experimental investigation of nanofluids on sintered heat pipe thermal performance, Appl. Therm. Eng. 29 (2009) 973–979.

[8] Z. Liu, J. Xiong, R. Bao, Boiling heat transfer characteristics of nanofluids in a flat heat pipe evaporator with micro-grooved heating surface, Int. J. Multiphase Flow 33 (2007) 1284–1295.

[9] R.R. Riehl, Analysis of loop heat pipe behavior using nanofluid, in: Heat Powered Cycles International Conference (HPC), New Castle, UK, 2006, Paper 06102.

[10] Y. Chen, W. Wei, S. Kang, C. Yu, Effect of nanofluid on flat heat pipe thermal performance, in: 24th IEEE SEMI-THERM Symposium, 2008, pp. 16–19.

[11] H.B. Ma, C. Wilson, B. Borgmeyer, K. Park, Q. Yu, S.U.S. Choi, M. Tirumala, Effect of nanofluid on the heat transport capability in an oscillating heat pipe, Appl. Phys. Lett. 88 (2006) 143116.

[12] Y. Lin, S. Kang, H. Chen, Effect of silver nanofluid on pulsating heat pipe thermal performance, Appl. Therm. Eng. 28 (2008) 1312–1317.

[13] C.Y. Tsaia, H.T. Chiena, P.P. Dingb, B. Chanc, T.Y. Luhd, P.H. Chena, Effect of structural character of gold nanoparticles in nanofluid on heat pipe thermal performance, Mater. Lett. 58 (2004) 1461–1465.

[14] G. Huminic, A. Huminic, Conjugate heat transfer in devices with nanoparticles, in: International Conference on Advanced Computational Engineering and Experimenting, ISSN 0933-5137, Barcelona, 2008, p. 188.

[15] G. Huminic, A. Huminic, CFD study of the heat pipes with water – nanoparticles mixture, in: Proceeding of European Automotive Simulation Conference, EASC 2009, Munich, 2009, pp. 217–228.

[16] G. Huminic, A. Huminic, Study on thermal performances of the heat pipes with water – nanoparticles mixture, in: Proceedings of World Congress Automotive, Detroit, Paper number 2010-01-0183, ISSN 1359-4311, 2010.

[17] M. Shafahi, V. Bianco, K. Vafai, O. Manca, An investigation of the thermal performance of cylindrical heat pipes using nanofluids, Int. J. Heat Mass Transfer 53 (2010) 376–383.

[18] T. Paramatthanuwat, S. Boothaisong, S. Rittidech, K. Booddachan, Heat transfer characteristics of a two-phase closed thermosyphon using de ionized water mixed with silver nano, Heat Mass Transfer 46 (2010) 281–285, doi:10.1007/s00231-009-0565-y.

[19] B. Mehta, S. Khandekar, Two-phase closed thermosyphon with nanofluids, in: 14th International Heat Pipe Conference, Brazil, 2007.

[20] S.H. Noie, S. Zeinali Heris, M. Kahani, S.M. Nowee, Heat transfer enhancement using Al2O3/water nanofluid in a two-phase closed thermosyphon, Int. J. Heat Fluid Flow 30 (2009) 700–705.

[21] A.E. Vol, Structure and Properties of Binary Metallic Systems, vol. 2, Fizmatgiz, Moscow, 1962.

[22] I. Morjan, R. Alexandrescu, F. Dumitrache, R. Birjega, C. Fleaca, I. Soare, C.R. Luculescu, G. Filoti, V. Kuncer, L. Vekas, N.C. Popa, G. Prodan, Iron oxide – based nanoparticles with different mean sizes obtained by the laser pyrolysis: structural and magnetic properties, J. Nanosci. Nanotechnol. 10 (2010), doi:10.1166/jnn.2010.1863.

[23] J.G. Collier, J.R. Thome, Convective Boiling and Condensation, Clarendon Press, Oxford, 1996.